Title

Capturing the sequence of events during the water oxidation reaction in photosynthesis using XFELs

Journal

FEBS Letters, 597(1)

ISSN

0014-5793

Authors

Simon, Philipp S

Makita, Hiroki

Bogacz, Isabel

et al.

Publication Date

2023

DOI

10.1002/1873-3468.14527

Peer reviewed

HHS Public Access

Author manuscript

FEBS Lett. Author manuscript; available in PMC 2024 January 01.

Published in final edited form as:

FEBS Lett. 2023 January ; 597(1): 30–37. doi:10.1002/1873-3468.14527.

Capturing the sequence of events during the water oxidation reaction in photosynthesis using XFELs

Philipp S. Simon[1], **Hiroki Makita**[1], **Isabel Bogacz**[1], **Franklin Fuller**[2], **Asmit Bhowmick**[1], **Rana Hussein**[3], **Mohamed Ibrahim**[3], **Miao Zhang**[1], **Ruchira Chatterjee**[1], **Mun Hon Cheah**[4], **Petko Chernev**[4], **Margaret Doyle**[1], **Aaron S. Brewster**[1], **Roberto Alonso-Mori**[5], **Nicholas K. Sauter**[1], **Uwe Bergmann**[6], **Holger Dobbek**[3], **Athina Zouni**[3], **Johannes Messinger**[4,7], **Jan Kern**[1], **Vittal K. Yachandra**[1], **Junko Yano**[1]

[1]Molecular Biophysics and Integrated Bioimaging Division, Lawrence Berkeley National Laboratory, Berkeley, CA 94720, USA.

[2]Pulse Institute, SLAC National Accelerator Laboratory, Menlo Park, CA 94025.

[3]Institut für Biologie, Humboldt-Universität zu Berlin, 10115 Berlin, Germany.

[4]Department of Chemistry - Ångström Laboratory, Molecular Biomimetics, Uppsala University, SE 75120 Uppsala, Sweden.

[5]LINAC Coherent Light Source, SLAC National Accelerator Laboratory, Menlo Park, CA 94025.

[6]Department of Physics, University of Wisconsin-Madison, Madison, WI, 53706, USA

[7]Department of Chemistry, Umeå University, SE 90187 Umeå, Sweden.

Abstract

Ever since the discovery that Mn was required for oxygen evolution in plants by Pirson in 1937 and the period-four oscillation in flash-induced oxygen evolution by Joliot and Kok in the 1970s, understanding of this process has advanced enormously using state-of-the-art methods. The most recent in this series of innovative techniques was the introduction of X-ray free electron lasers (XFELs) a decade ago, which led to another quantum leap in the understanding in this field, by enabling operando X-ray structural and X-ray spectroscopy studies at room temperature. This review summarizes the current understanding of the structure of Photosystem II (PS II) and its catalytic center, the Mn_4CaO_5 complex, in the intermediate S_i(i=0–4)-states of the Kok cycle, as obtained using XFELs.

Graphical Abstract

Water oxidation reaction in nature is catalyzed by the Mn_4CaO_5 cluster in Photosystem II. We have developed operando X-ray crystallography and X-ray spectroscopy methods at the X-ray free electron laser facilities and applied it to understand the catalytic mechanism and associated protein dynamics in Photosystem II.

Funding sources and disclosure of conflicts of interest

Funding sources are in the acknowledgements. There are no conflicts of interest.

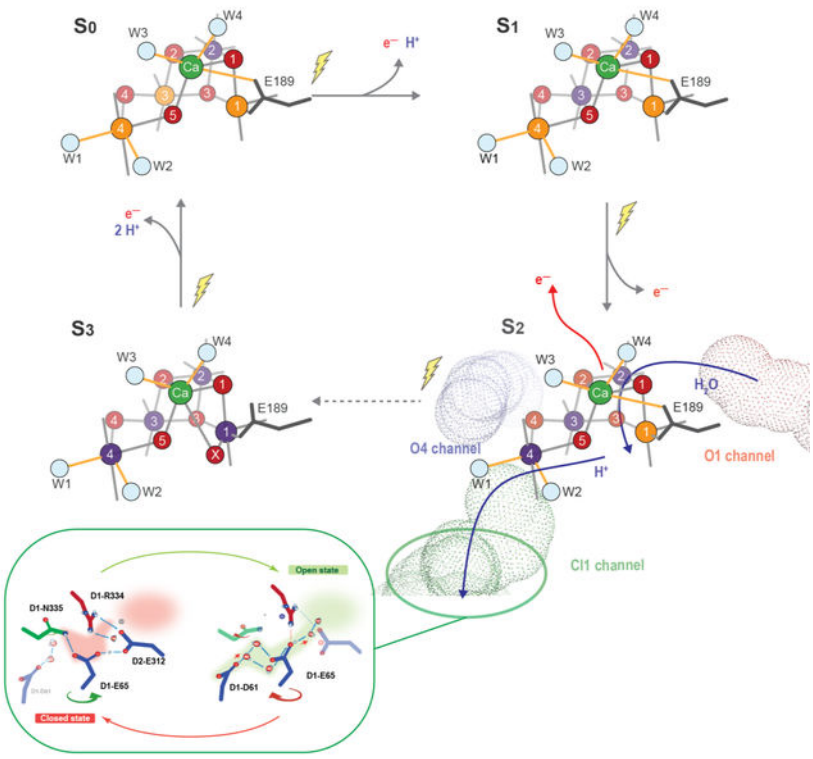

Keywords

photosystem II; oxygen evolving complex; manganese metalloenzymes; water-oxidation/splitting; X-ray free electron laser; X-ray spectroscopy

Introduction to the water oxidation reaction in photosynthesis

The water oxidation reaction in nature is carried out by Photosystem II (PS II), a multisubunit membrane protein complex. This light-driven reaction is made possible by a series of spatially separated cofactors that extends over 40 Å, and includes the donor (the Mn_4CaO_5 catalytic center), the reaction center chlorophylls, and ends with the mobile quinone electron acceptor (Q_B) [1,2]. Such chemical architecture provides an ideal platform to investigate the coupling of the one-electron charge separation reactions at the pico-second time scale with multi-electron/proton chemistry occurring at the millisecond time scale, using earth-abundant metal cofactors embedded in a flexible protein-water network. Understanding the insights from nature's design provides inspiration for how to build artificial photosynthetic devices, where the controlled accumulation of charge and high-selectivity of products, is currently challenging, especially if the catalysts are made of earth-abundant elements.

To solve the mechanism of the water oxidation reaction in PS II, our strategy has been to follow the structural and chemical sequence of events in the enzyme that lead to O-O

bond formation, and to understand the cycle of the catalytic reaction at the atomic and electronic structure levels. The questions regarding this light-driven water oxidation reaction include: What structural parameters control reaction kinetics? How does the environment (protein and hydrogen-bonding network) change to accommodate a dynamically evolving energy landscape during the multielectron/multiproton chemistry, while adjusting local pH and redox potential to drive chemistry? What are the features of PS II that activate the earth abundant metals Mn and Ca, which are the building blocks of the catalytic center of water oxidation in PS II, so that they can support highly efficient water oxidation catalysis? To answer these questions, application of new methods in crystallography and X-ray spectroscopy at X-ray free electron lasers (XFELs) plays a critical role.

X-ray free electron lasers enable mechanistic studies of Photosystem II

The X-ray pulses generated by an XFEL are extremely intense with short pulse widths, containing as many photons (10^{12}) in one pulse (<50 femtoseconds) as synchrotron beam lines provide in one second [3,4]. Moreover, the X-ray beam is very small in size, typically 2–5 microns or in some instances 100 nm in width, and therefore the sample/crystals being studied can be very small. These unique properties of the XFEL pulses make it possible to perform shot-by-shot X-ray data collection at room temperature: the femtosecond pulse is faster than the diffusion of radicals (picoseconds) caused by the X-rays in biological samples [5–7], and therefore the data can be collected before radiation-induced sample changes can develop, even at room temperature. This capability has made it possible to follow the structural and chemical changes in PS II in real time, as the reaction proceeds [8–10]. In PS II, this implies that one can access the reaction process at physiological temperature and of particular interest is the S_3 to S_0 transition via the transient S_4 state; a step during which O-O bond formation, evolution of molecular oxygen, and substrate water binding occur. Unlike the stable intermediates (S_0 to S_3 states), the transient S_4 state and the transients between successive S-states cannot be cryo-trapped, and therefore need to be studied at room temperature in a time-resolved manner.

To take full advantage of the capability of XFELs for the mechanistic studies of PS II, there have been several challenges that arise from the fact that at XFELs the sample is destroyed after each X-ray pulse. Establishing methods for preparing large volumes of suspension of highly-diffracting microcrystals of defined size, delivering these samples efficiently at the rate of XFELs, *in situ* photoexcitation, and fast data analysis providing real-time feedback have been prime requirements [5,6,8,9,10]. While many different approaches using liquid jets [12–15] or rastering of solid targets [16,17] (see also [18–20] for general reviews on sample delivery) have been utilized so far to deliver PS II samples to the X-ray beam each of them had shortcomings, for example in terms of sample consumption, illumination precision or available measurement modes. To circumvent these, we developed a robust drop-on-demand sample delivery setup for room temperature X-ray crystallography/X-ray emission spectroscopy (XES), with photochemical triggers to advance the S-states *in situ* (Fig. 1) [21]. Droplets that contain protein crystal suspension are formed by an acoustic droplet ejector that is connected to the sample well and that is automatically re-filled via a Hamilton syringe driven by a syringe pump. Typically, the droplets have a size of ~ 150 – 200 μm and contain several dozens of PS II single crystals (10 – 50 μm size). With this

setup, we routinely achieve a droplet hit rate of close to 100% and a crystal hit rate of ~ 20–50%. Images with occasional multiple crystal hits can be deconvoluted and analyzed separately. The setup allows us to take snapshots of crystallography and XES data with a pump-probe time delay between ~100 fs and up to several 10s of msecs and we can cycle PS II through its reaction cycle by exposing each single droplet to 1, 2, 3 or 4 light flashes before X-ray exposure. Using this setup [22,23] as well as other approaches [10,15], XFEL studies have started revealing the details of how water is oxidized by PS II and the role of the protein environment in the process. Below we discuss the interplay of structural changes of the overall protein and the chemical changes occurring at the metal-site as PS II cycles through the enzymatic reaction.

Fig. 2 shows the stepwise changes of the electron density at the oxygen evolving complex (OEC) during the oxygen-evolving cycle, that are captured using the setup shown in Fig. 1. The electron density map ($2mF_{obs} - DF_{calc}$, green to blue) and O5/Ox omit map density (pink to red) of the 0F-3F states (measured 200 msec after illumination of the sample by 0, 1, 2 or 3 light flashes, respectively) are overlaid. The 0F and 1F data have a dominant population (> 90%) of the S_1 and S_2 state, respectively, and therefore they are considered as containing only a single species. On the other hand, 2F and 3F data are more mixed due to PS II's intrinsic miss parameters, that lead to a desynchronization of the states [9,22,24]. The S-state population of these flash states are estimated via *ex situ* methods of the same sample (electron paramagnetic resonance spectroscopy (EPR) and membrane inlet mass spectrometry (MIMS)) [25,26] as well as an *in situ* method (XES), that is carried out simultaneously with X-ray crystallography [27]. Based on the population analysis, we extracted pure S-state structures from the flashed data, which are shown along with the electron density map of the flashed states in Fig. 2. The likely assignment of Mn oxidation states (Mn^{3+} is depicted in orange, Mn^{4+} in purple) as well as protonation and deprotonation reactions are indicated for each S state. In the S_1 state, the cluster is in a distinct 'right-open' structure with no bond between Mn1 and O5; the Mn4–O5 distance is about 2.2 Å, whereas the Mn1–O5 distance is about 2.7 Å, with Mn1 in a pentacoordinate ligand environment. Upon the transition from S_1 to S_2, the structure of the cluster remains fundamentally unchanged, but one Mn, likely Mn4, is oxidized from +3 to +4. The S_3 state is unique as Mn1 has gained an additional, sixth oxygen ligand that forms a bridge between Mn1 and Ca.

To understand the sequence of events leading to the insertion of this new oxygen bridge, we recorded diffraction and Mn Kβ XES data at several time points during the $S_2 \rightarrow S_3$ transition. We observed that the tyrosine Y_Z residue, located between the reaction center chlorophylls and the OEC, shows some movement by 50 μs after the 2nd flash, along with the His190 residue that is hydrogen-bonded to Yz. Then, the Glu189 side chain, which bridges Mn1 and Ca and is located close to His190, moves away from Ca. This is followed by Mn1 and Mn4 moving apart as the extra oxygen bridge (O_X(H)) is inserted at the open coordination site of Mn1 and Ca. Our structural data indicate that Ox could be supplied via a "water wheel" like arrangement of five waters next to the OEC that is connected by the 'O1 channel' (see Fig. 3) to the bulk solvent. We hypothesize that the Ca coordination environment, for example W4 →W3 →Ox, is used as a path for the water insertion to Mn1. XES spectra show that Mn oxidation (τ of ~350 μs) during the $S_2 \rightarrow S_3$ transition mirrors the appearance of O_X electron density, showing that insertion happens in parallel to Mn1

oxidation from Mn^{3+} to Mn^{4+}. Thus, in S_3 all four Mn seem to be oxidized to a formal oxidation state of 4+ [8].

Upon the 3rd flash, the S_3 state advances to the S_0 state, which shows the original right-open configuration of the cluster (Fig. 2), but with one of the Mn-Mn distances (Mn3-Mn4) slightly elongated due to the presence of Mn^{3+} and the protonation of one μ-oxo bridge. During this reaction step, O_2 is formed and released, and one additional water needs to bind to restore the Mn_4CaO_5 cluster. In addition, two protons are released, one before O-O formation and one concomitant with O_2 release and water binding [1,22,28,29]. These reactions steps are presently being studied by XFEL.

The ability to advance the reaction through the Kok cycle *in situ*, evidenced by the crystallography and X-ray spectroscopy results at XFELs [8,9], provides evidence that PS II reaction centers are fully active in the crystalline environment under the physiological temperature that is used during the experiments (Fig. 1). In addition, it demonstrates that our efficient drop-on-demand sample delivery to the X-ray intersection points (Fig. 1), which avoids dehydrating crystals, efficiently prevents the loss of enzyme activity, decrease of diffractivity, and the release of Mn^{2+}. There has been a debate of whether multiple OEC configurations exists in each S-state due to spin isomerization and/or different protonation states of oxygens [30–32]. Determining positions of heavy atoms like Mn is highly accurate at the current resolution of 2.0 Å, and no clear evidence of multiple metal positions were observed in each S-state. On the other hand, the expected structural differences between multiple oxygen positions due to different protonation states are more subtle and require higher resolution diffraction data. We, however, note that within our lower detection limit of ~ 10% of the population, the S-state models shown in Fig. 1 are the dominant configuration, and the minority fractions, if they exist, will not be accurately detected at the current crystallography resolution of ~2.0 Å.

Besides the function of the catalytic center, the importance of the protein environment, including the hydrogen bonding network, has been recognized more and more in the field of bioinorganic catalysis. In PS II, water and proton pathways are required to facilitate substrate delivery to and proton egress from the catalytic site. Such channels have been proposed from theoretical studies built on the crystallography data [33–38]. Out of the three main channels - ‘O1 channel’, ‘Cl1 channel’ and ‘O4 channel’ - identified in the room temperature structures (Fig. 3), recent structural studies propose that the O1 channel is the likely water intake pathway [8,39]. This hypothesis is based on the high mobility of waters located along the O1 channel. On the other hand, the Cl1 channel is the likely proton release pathway in this transition, based on the structural rearrangements of water molecules and amino acid side chains along these channels [8,39]. The reversible rotation of the amino acid residue D1-E65 is observed in the time resolved room temperature data (Fig. 3 bottom), and it is hypothesized that this area serves as a gate for proton transport that plays a role in minimizing the back reaction [39]. The results indicate that the water oxidation reaction at the OEC is well coordinated with the amino acid side chains and the hydrogen-bonding network over the entire length of the channels, which is essential in shuttling substrate waters and protons. A similar study is necessary for the other S-state

transitions, in particular, for the S_3 to S_0 transition where the catalytic center resets the process by four electron reduction of the Mn_4CaO_6 cluster, along with O_2 release.

Conclusions and perspectives

The progress of the room temperature structural insights into PS II and its catalytic mechanism summarized here is based on more than a decade-long development of the XFEL-based X-ray methods, and more specifically the development of sample preparation [40] and sample introduction methods into the X-ray pulses with multiple-illumination protocols required for PS II samples [21], and constant improvements on analysis methods for serial crystallography data from XFELs [41][42][43]. The first decade of XFEL science has brought us many striking results and the emergence of exciting new research fields in the biosciences area. However, much work still lies ahead when it comes to making the best use of this powerful tool. Similar concepts have been applied for other metalloenzyme reaction studies that are triggered by mixing with a gas or by chemical mixing with a substrate [21,44,45]. Understanding the function of metalloenzymes, which are very important in the field of human health and of relevance to renewable energy, will greatly benefit from current and future XFELs and the X-ray methods described that make it possible to follow the atomic and electronic structural changes, in real time, at room temperature, as the metalloenzymes progress through the catalytic reactions.

Acknowledgements

This work was supported by the Director, Office of Science, Office of Basic Energy Sciences (OBES), Division of Chemical Sciences, Geosciences, and Biosciences (CSGB) of the Department of Energy (DOE) (J.Y., V.K.Y., J.K.) for X-ray spectroscopy and crystallography data collection and analysis, and methods development for photosynthetic systems, by the National Institutes of Health (NIH) Grants GM055302 (V.K.Y.) for PS II biochemistry, GM110501 (J.Y.) and GM126289 (J.K.) for instrumentation development for XFEL experiments, GM117126 (N.K.S.) for development of computational protocols for XFEL data. N.K.S acknowledges support from the Exascale Computing Project (grant 17-SC20-SC), a collaborative effort of the DOE Office of Science and the National Nuclear Security Administration. Germany's Excellence Strategy (Project EXC 2008/1-390540038 (A.Z., H.D.) coordinated by T.U. Berlin and by the German Research Foundation (DFG) via the Collaborative Research Center SFB1078 (Humboldt Universität zu Berlin), TP A5 (A.Z., H.D., M.I., R.H.) and Vetenskapsrådet 2016-05183 (J.M.) and 2020-03809 (J.M.), as well as Energimyndigheten 45421-1 (J.M.) are acknowledged for support. R.H. acknowledges support by a Caroline von Humboldt Stipendium, Humboldt University Berlin. This research used resources of NERSC, a User Facility supported by the Office of Science, DOE, under Contract No. DE-AC02-05CH11231. XFEL data was collected at LCLS/SLAC, Stanford and SACLA, Japan. Testing of crystals and various parts of the setup was carried out at synchrotron facilities that were provided by the ALS in Berkeley and SSRL in Stanford, funded by DOE OBES. The SSRL Structural Molecular Biology Program is supported by the DOE OBER, and by the NIH (P41GM103393). Use of the LCLS and SSRL, SLAC National Accelerator Laboratory, is supported by the U.S. DOE, Office of Science, OBES under Contract No. DE-AC02-76SF00515. We thank the support staff at LCLS/SLAC, SACLA/Japan, SSRL and ALS.

Abbreviations:

EPR	electron paramagnetic resonance spectroscopy
MIMS	membrane inlet mass spectrometry
XAS	X-ray absorption spectroscopy
XES	X-ray emission spectroscopy
XFEL	X-ray free electron laser

DOT	drop-on-tape method
XRD	X-ray diffraction

References

1. Hillier W, and Messinger J (2005) Mechanism of photosynthetic oxygen production, in Photosystem II: The light-driven water:plastoquinone oxidoreductase, eds. Wydrzynski T, Satoh K, Springer.
2. Shevela D, Kern JF, Govindjee G, Whitmarsh J, and Messinger J (2021) Photosystem II, in eLS, John Wiley & Sons, Ltd, pp. 1–16.
3. Bergmann U, Kern J, Schoenlein RW, Wernet P, Yachandra VK, and Yano J (2021) Using X-ray free-electron lasers for spectroscopy of molecular catalysts and metalloenzymes. Nature Reviews Physics.
4. Margaritondo G, and Rebernik Ribic P (2011) A simplified description of X-ray free-electron lasers. J Synchrotron Radiat, 18 (Pt 2), 101–8. [PubMed: 21335894]
5. Barty A, Caleman C, Aquila A, Timneanu N, Lomb L, White TA, Andreasson J, Arnlund D, Bajt S, Barends TRM, Barthelmess M, Bogan MJ, Bostedt C, Bozek JD, Coffee R, Coppola N, Davidsson J, DePonte DP, Doak RB, Ekeberg T, Elser V, Epp SW, Erk B, Fleckenstein H, Foucar L, Fromme P, Graafsma H, Gumprecht L, Hajdu J, Hampton CY, Hartmann R, Hartmann A, Hauser G, Hirsemann H, Holl P, Hunter MS, Johansson L, Kassemeyer S, Kimmel N, Kirian RA, Liang M, Maia FRNC, Malmerberg E, Marchesini S, Martin AV, Nass K, Neutze R, Reich C, Rolles D, Rudek B, Rudenko A, Scott H, Schlichting I, Schulz J, Seibert MM, Shoeman RL, Sierra RG, Soltau H, Spence JCH, Stellato F, Stern S, Strüder L, Ullrich J, Wang X, Weidenspointner G, Weierstall U, Wunderer CB, and Chapman HN (2012) Self-terminating diffraction gates femtosecond X-ray nanocrystallography measurements. Nature Photon, 6 (1), 35–40.
6. Lomb L, Barends TRM, Kassemeyer S, Aquila A, Epp SW, Erk B, Foucar L, Hartmann R, Rudek B, Rolles D, Rudenko A, Shoeman RL, Andreasson J, Bajt S, Barthelmess M, Barty A, Bogan MJ, Bostedt C, Bozek JD, Caleman C, Coffee R, Coppola N, DePonte DP, Doak RB, Ekeberg T, Fleckenstein H, Fromme P, Gebhardt M, Graafsma H, Gumprecht L, Hampton CY, Hartmann A, Hauser G, Hirsemann H, Holl P, Holton JM, Hunter MS, Kabsch W, Kimmel N, Kirian RA, Liang M, Maia FRNC, Meinhart A, Marchesini S, Martin AV, Nass K, Reich C, Schulz J, Seibert MM, Sierra R, Soltau H, Spence JCH, Steinbrener J, Stellato F, Stern S, Timneanu N, Wang X, Weidenspointner G, Weierstall U, White TA, Wunderer C, Chapman HN, Ullrich J, Strüder L, and Schlichting I (2011) Radiation damage in protein serial femtosecond crystallography using an x-ray free-electron laser. Phys. Rev. B, 84 (21), 214111.
7. Neutze R, Wouts R, and Hajdu J (2000) Potential for biomolecular imaging with femtosecond X-ray pulses. 406, 6.
8. Ibrahim M, Fransson T, Chatterjee R, Cheah MH, Hussein R, Lassalle L, Sutherlin KD, Young ID, Fuller FD, Gul S, Kim I-S, Simon PS, de Lichtenberg C, Chernev P, Bogacz I, Pham CC, Orville AM, Saichek N, Northen T, Batyuk A, Carbajo S, Alonso-Mori R, Tono K, Owada S, Bhowmick A, Bolotovsky R, Mendez D, Moriarty NW, Holton JM, Dobbek H, Brewster AS, Adams PD, Sauter NK, Bergmann U, Zouni A, Messinger J, Kern J, Yachandra VK, and Yano J (2020) Untangling the sequence of events during the $S_2 \rightarrow S_3$ transition in photosystem II and implications for the water oxidation mechanism. Proc. Natl. Acad. Sci. U.S.A, 117 (23), 12624–12635. [PubMed: 32434915]
9. Kern J, Chatterjee R, Young ID, Fuller FD, Lassalle L, Ibrahim M, Gul S, Fransson T, Brewster AS, Alonso-Mori R, Hussein R, Zhang M, Douthit L, de Lichtenberg C, Cheah MH, Shevela D, Wersig J, Seuffert I, Sokaras D, Pastor E, Weninger C, Kroll T, Sierra RG, Aller P, Butryn A, Orville AM, Liang M, Batyuk A, Koglin JE, Carbajo S, Boutet S, Moriarty NW, Holton JM, Dobbek H, Adams PD, Bergmann U, Sauter NK, Zouni A, Messinger J, Yano J, and Yachandra VK (2018) Structures of the intermediates of Kok's photosynthetic water oxidation clock. Nature, 563 (7731), 421–425. [PubMed: 30405241]
10. Suga M, Akita F, Yamashita K, Nakajima Y, Ueno G, Li H, Yamane T, Hirata K, Umena Y, Yonekura S, Yu L-J, Murakami H, Nomura T, Kimura T, Kubo M, Baba S, Kumasaka T, Tono K, Yabashi M, Isobe H, Yamaguchi K, Yamamoto M, Ago H, and Shen J-R (2019) An oxyl/oxo

mechanism for oxygen-oxygen coupling in PSII revealed by an x-ray free-electron laser. Science, 366 (6463), 334–338. [PubMed: 31624207]

11. Chatterjee R, Lassalle L, Gul S, Fuller FD, Young ID, Ibrahim M, de Lichtenberg C, Cheah MH, Zouni A, Messinger J, Yachandra VK, Kern J, and Yano J (2019) Structural isomers of the S_2 state in photosystem II: do they exist at room temperature and are they important for function? Physiol Plantarum, 166 (1), 60–72.
12. Sierra RG, Laksmono H, Kern J, Tran R, Hattne J, Alonso-Mori R, Lassalle-Kaiser B, Glockner C, Hellmich J, Schafer DW, Echols N, Gildea RJ, Grosse-Kunstleve RW, Sellberg J, McQueen TA, Fry AR, Messerschmidt MM, Miahnahri A, Seibert MM, Hampton CY, Starodub D, Loh ND, Sokaras D, Weng TC, Zwart PH, Glatzel P, Milathianaki D, White WE, Adams PD, Williams GJ, Boutet S, Zouni A, Messinger J, Sauter NK, Bergmann U, Yano J, Yachandra VK, and Bogan MJ (2012) Nanoflow electrospinning serial femtosecond crystallography. Acta Crystallogr D Biol Crystallogr, 68 (Pt 11), 1584–7. [PubMed: 23090408]
13. Kupitz C, Basu S, Grotjohann I, Fromme R, Zatsepin NA, Rendek KN, Hunter MS, Shoeman RL, White TA, Wang D, James D, Yang JH, Cobb DE, Reeder B, Sierra RG, Liu H, Barty A, Aquila AL, Deponte D, Kirian RA, Bari S, Bergkamp JJ, Beyerlein KR, Bogan MJ, Caleman C, Chao TC, Conrad CE, Davis KM, Fleckenstein H, Galli L, Hau-Riege SP, Kassemeyer S, Laksmono H, Liang M, Lomb L, Marchesini S, Martin AV, Messerschmidt M, Milathianaki D, Nass K, Ros A, Roy-Chowdhury S, Schmidt K, Seibert M, Steinbrener J, Stellato F, Yan L, Yoon C, Moore TA, Moore AL, Pushkar Y, Williams GJ, Boutet S, Doak RB, Weierstall U, Frank M, Chapman HN, Spence JC, and Fromme P (2014) Serial time-resolved crystallography of photosystem II using a femtosecond X-ray laser. Nature, 513 (7517), 261–5. [PubMed: 25043005]
14. Sierra RG, Gati C, Laksmono H, Dao EH, Gul S, Fuller F, Kern J, Chatterjee R, Ibrahim M, Brewster AS, Young ID, Michels-Clark T, Aquila A, Liang M, Hunter MS, Koglin JE, Boutet S, Junco EA, Hayes B, Bogan MJ, Hampton CY, Puglisi EV, Sauter NK, Stan CA, Zouni A, Yano J, Yachandra VK, Soltis SM, Puglisi JD, and DeMirci H (2016) Concentric-flow electrokinetic injector enables serial crystallography of ribosome and photosystem II. Nat Methods, 13 (1), 59–62. [PubMed: 26619013]
15. Suga M, Akita F, Sugahara M, Kubo M, Nakajima Y, Nakane T, Yamashita K, Umena Y, Nakabayashi M, Yamane T, Nakano T, Suzuki M, Masuda T, Inoue S, Kimura T, Nomura T, Yonekura S, Yu L-J, Sakamoto T, Motomura T, Chen J-H, Kato Y, Noguchi T, Tono K, Joti Y, Kameshima T, Hatsui T, Nango E, Tanaka R, Naitow H, Matsuura Y, Yamashita A, Yamamoto M, Nureki O, Yabashi M, Ishikawa T, Iwata S, and Shen J-R (2017) Light-induced structural changes and the site of O=O bond formation in PSII caught by XFEL. Nature, 543 (7643), 131–135. [PubMed: 28219079]
16. Baxter EL, Aguila L, Alonso-Mori R, Barnes CO, Bonagura CA, Brehmer W, Brunger AT, Calero G, Caradoc-Davies TT, Chatterjee R, Degrado WF, Fraser JS, Ibrahim M, Kern J, Kobilka BK, Kruse AC, Larsson KM, Lemke HT, Lyubimov AY, Manglik A, McPhillips SE, Norgren E, Pang SS, Soltis SM, Song J, Thomaston J, Tsai Y, Weis WI, Woldeyes RA, Yachandra V, Yano J, Zouni A, and Cohen AE (2016) High-density grids for efficient data collection from multiple crystals. Acta Crystallogr D Struct Biol, 72 (Pt 1), 2–11. [PubMed: 26894529]
17. Suga M, Akita F, Hirata K, Ueno G, Murakami H, Nakajima Y, Shimizu T, Yamashita K, Yamamoto M, Ago H, and Shen JR (2015) Native structure of photosystem II at 1.95 Å resolution viewed by femtosecond X-ray pulses. Nature, 517 (7532), 99–103. [PubMed: 25470056]
18. Martiel I, Müller-Werkmeister HM, and Cohen AE (2019) Strategies for sample delivery for femtosecond crystallography. Acta Crystallographica Section D Structural Biology, 75 (2), 160–177. [PubMed: 30821705]
19. Deponte D (2017) Sample Delivery Methods: Liquids and Gases at FELs, in X-Ray Free Electron Lasers: Applications in Materials, Chemistry and Biology (eds.Bergmann U, Yachandra VK, and Yano J), Royal Society of Chemistry, London, UK, pp. 325–336.
20. Barends TRM, Stauch B, Cherezov V, and Schlichting I (2022) Serial femtosecond crystallography. Nat Rev Methods Primers, 2 (1), 1–24.
21. Fuller FD, Gul S, Chatterjee R, Burgie ES, Young ID, Lebrette H, Srinivas V, Brewster AS, Michels-Clark T, Clinger JA, Andi B, Ibrahim M, Pastor E, de Lichtenberg C, Hussein R, Pollock CJ, Zhang M, Stan CA, Kroll T, Fransson T, Weninger C, Kubin M, Aller P, Lassalle L, Bräuer P,

Miller MD, Amin M, Koroidov S, Roessler CG, Allaire M, Sierra RG, Docker PT, Glownia JM, Nelson S, Koglin JE, Zhu D, Chollet M, Song S, Lemke H, Liang M, Sokaras D, Alonso-Mori R, Zouni A, Messinger J, Bergmann U, Boal AK, Bollinger JM, Krebs C, Högbom M, Phillips GN, Vierstra RD, Sauter NK, Orville AM, Kern J, Yachandra VK, and Yano J (2017) Drop-on-demand sample delivery for studying biocatalysts in action at X-ray free-electron lasers. Nat Methods, 14 (4), 443–449. [PubMed: 28250468]

22. Renger G (2012) Mechanism of light induced water splitting in Photosystem II of oxygen evolving photosynthetic organisms. Biochim. Biophys. Acta Bioenerg, 1817 (8), 1164–76.
23. Bernat G, Morvaridi F, Feyziyev Y, and Styring S (2002) pH dependence of the four individual transitions in the catalytic S-cycle during photosynthetic oxygen evolution. Biochemistry, 41 (18), 5830–43. [PubMed: 11980487]
24. Han G, Chernev P, Styring S, Messinger J, and Mamedov F (2022) Molecular basis for turnover inefficiencies (misses) during water oxidation in photosystem II. Chem. Sci, 13 (29), 8667–8678. [PubMed: 35974765]
25. Beckmann K, Messinger J, Badger MR, Wydrzynski T, and Hillier W (2009) On-line mass spectrometry: membrane inlet sampling. Photosynth Res, 102 (2–3), 511–522. [PubMed: 19653116]
26. Fransson T, Chatterjee R, Fuller FD, Gul S, Weninger C, Sokaras D, Kroll T, Alonso-Mori R, Bergmann U, Kern J, Yachandra VK, and Yano J (2018) X-ray Emission Spectroscopy as an *in Situ* Diagnostic Tool for X-ray Crystallography of Metalloproteins Using an X-ray Free-Electron Laser. Biochemistry, 57 (31), 4629–4637. [PubMed: 29906115]
27. Kern J, Alonso-Mori R, Tran R, Hattne J, Gildea RJ, Echols N, Glöckner C, Hellmich J, Laksmono H, Sierra RG, Lassalle-Kaiser B, Koroidov S, Lampe A, Han G, Gul S, DiFiore D, Milathianaki D, Fry AR, Miahnahri A, Schafer DW, Messerschmidt M, Seibert MM, Koglin JE, Sokaras D, Weng T-C, Sellberg J, Latimer MJ, Grosse-Kunstleve RW, Zwart PH, White WE, Glatzel P, Adams PD, Bogan MJ, Williams GJ, Boutet S, Messinger J, Zouni A, Sauter NK, Yachandra VK, Bergmann U, and Yano J (2013) Simultaneous Femtosecond X-ray Spectroscopy and Diffraction of Photosystem II at Room Temperature. Science, 340 (6131), 491–495. [PubMed: 23413188]
28. Cox N, and Messinger J (2013) Reflections on substrate water and dioxygen formation. Biochim. Biophys. Acta, 1827 (8–9), 1020–30. [PubMed: 23380392]
29. Klauss A, Haumann M, and Dau H (2015) Seven steps of alternating electron and proton transfer in photosystem II water oxidation traced by time-resolved photothermal beam deflection at improved sensitivity. J. Phys. Chem. B, 119 (6), 2677–89. [PubMed: 25402235]
30. Pantazis DA, Ames W, Cox N, Lubitz W, and Neese F (2012) Two interconvertible structures that explain the spectroscopic properties of the oxygen-evolving complex of photosystem II in the S_2 state. Angew. Chem. Int. Ed, 51 (39), 9935–40.
31. Boussac A, Ugur I, Marion A, Sugiura M, Kaila VRI, and Rutherford AW (2018) The low spin - high spin equilibrium in the S2-state of the water oxidizing enzyme. Biochimica et Biophysica Acta (BBA) - Bioenergetics, 1859 (5), 342–356. [PubMed: 29499187]
32. Corry TA, and O'Malley PJ (2019) Proton Isomers Rationalize the High- and Low-Spin Forms of the S2 State Intermediate in the Water-Oxidizing Reaction of Photosystem II. J Phys Chem Lett, 5226–5230. [PubMed: 31429574]
33. Gabdulkhakov A, Guskov A, Broser M, Kern J, Müh F, Saenger W, and Zouni A (2009) Probing the Accessibility of the Mn4Ca Cluster in Photosystem II: Channels Calculation, Noble Gas Derivatization, and Cocrystallization with DMSO. Structure, 17 (9), 1223–1234. [PubMed: 19748343]
34. Ho FM (2008) Uncovering channels in photosystem II by computer modelling: current progress, future prospects, and lessons from analogous systems. Photosynth Res, 98 (1–3), 503–22. [PubMed: 18798008]
35. Vassiliev S, Zaraiskaya T, and Bruce D (2012) Exploring the energetics of water permeation in photosystem II by multiple steered molecular dynamics simulations. Biochimica et Biophysica Acta (BBA) - Bioenergetics, 1817 (9), 1671–1678. [PubMed: 22683291]
36. Vassiliev S, Zaraiskaya T, and Bruce D (2013) Molecular dynamics simulations reveal highly permeable oxygen exit channels shared with water uptake channels in photosystem II. Biochimica et Biophysica Acta (BBA) - Bioenergetics, 1827 (10), 1148–1155. [PubMed: 23816955]

37. Sakashita N, Watanabe HC, Ikeda T, Saito K, and Ishikita H (2017) Origins of Water Molecules in the Photosystem II Crystal Structure. Biochemistry, 56 (24), 3049–3057. [PubMed: 28534615]

38. Sakashita N, Ishikita H, and Saito K (2020) Rigidly hydrogen-bonded water molecules facilitate proton transfer in photosystem II. Phys. Chem. Chem. Phys, 22 (28), 15831–15841. [PubMed: 32613215]

39. Hussein R, Ibrahim M, Bhowmick A, Simon PS, Chatterjee R, Lassalle L, Doyle M, Bogacz I, Kim I-S, Cheah MH, Gul S, de Lichtenberg C, Chernev P, Pham CC, Young ID, Carbajo S, Fuller FD, Alonso-Mori R, Batyuk A, Sutherlin KD, Brewster AS, Bolotovsky R, Mendez D, Holton JM, Moriarty NW, Adams PD, Bergmann U, Sauter NK, Dobbek H, Messinger J, Zouni A, Kern J, Yachandra VK, and Yano J (2021) Structural dynamics in the water and proton channels of photosystem II during the S2 to S3 transition. Nat Commun, 12 (1), 6531. [PubMed: 34764256]

40. Ibrahim M, Chatterjee R, Hellmich J, Tran R, Bommer M, Yachandra VK, Yano J, Kern J, and Zouni A (2015) Improvements in serial femtosecond crystallography of photosystem II by optimizing crystal uniformity using microseeding procedures. Struct. Dyn, 2 (4).

41. Hattne J, Echols N, Tran R, Kern J, Gildea RJ, Brewster AS, Alonso-Mori R, Glockner C, Hellmich J, Laksmono H, Sierra RG, Lassalle-Kaiser B, Lampe A, Han G, Gul S, DiFiore D, Milathianaki D, Fry AR, Miahnahri A, White WE, Schafer DW, Seibert MM, Koglin JE, Sokaras D, Weng TC, Sellberg J, Latimer MJ, Glatzel P, Zwart PH, Grosse-Kunstleve RW, Bogan MJ, Messerschmidt M, Williams GJ, Boutet S, Messinger J, Zouni A, Yano J, Bergmann U, Yachandra VK, Adams PD, and Sauter NK (2014) Accurate macromolecular structures using minimal measurements from X-ray free-electron lasers. Nat Methods, 11 (5), 545–8. [PubMed: 24633409]

42. Brewster AS, Waterman DG, Parkhurst JM, Gildea RJ, Young ID, O'Riordan LJ, Yano J, Winter G, Evans G, and Sauter NK (2018) Improving signal strength in serial crystallography with DIALS geometry refinement. Acta Cryst. D, 74 (Pt 9), 877–894.

43. Sauter NK (2015) XFEL diffraction: developing processing methods to optimize data quality. J Synchrotron Radiat, 22 (2), 239–48. [PubMed: 25723925]

44. Butryn A, Simon PS, Aller P, Hinchliffe P, Massad RN, Leen G, Tooke CL, Bogacz I, Kim I-S, Bhowmick A, Brewster AS, Devenish NE, Brem J, Kamps JJAG, Lang PA, Rabe P, Axford D, Beale JH, Davy B, Ebrahim A, Orlans J, Storm SLS, Zhou T, Owada S, Tanaka R, Tono K, Evans G, Owen RL, Houle FA, Sauter NK, Schofield CJ, Spencer J, Yachandra VK, Yano J, Kern JF, and Orville AM (2021) An on-demand, drop-on-drop method for studying enzyme catalysis by serial crystallography. Nat Commun, 12 (1), 4461. [PubMed: 34294694]

45. Rabe P, Kamps J, Sutherlin KD, Linyard JDS, Aller P, Pham CC, Makita H, Clifton I, McDonough MA, Leissing TM, Shutin D, Lang PA, Butryn A, Brem J, Gul S, Fuller FD, Kim IS, Cheah MH, Fransson T, Bhowmick A, Young ID, O'Riordan L, Brewster AS, Pettinati I, Doyle M, Joti Y, Owada S, Tono K, Batyuk A, Hunter MS, Alonso-Mori R, Bergmann U, Owen RL, Sauter NK, Claridge TDW, Robinson CV, Yachandra VK, Yano J, Kern JF, Orville AM, and Schofield CJ (2021) X-ray free-electron laser studies reveal correlated motion during isopenicillin N synthase catalysis. Sci Adv, 7 (34), eabh0250. [PubMed: 34417180]

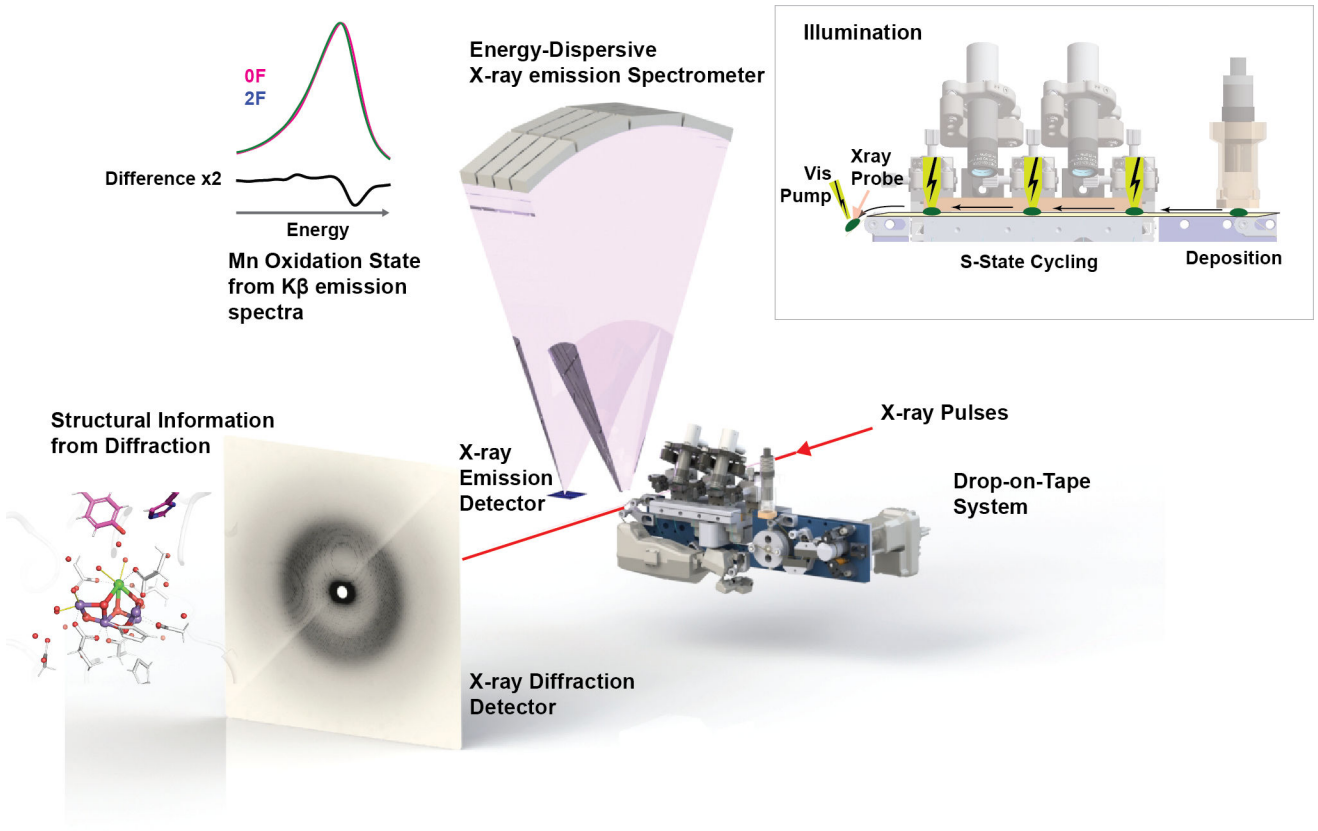

Figure 1. Setup for delivering protein crystal suspension to the X-ray intersection point to perform simultaneous X-ray crystallography and X-ray emission spectroscopy.

The Drop-on-Tape system (center) [21] uses acoustic pulses to generate nl-sized droplets of protein crystal suspensions which are deposited on a polyimide transport tape. The droplets are then illuminated by up to 3 laser flashes before being transported into the X-ray interaction region (top right). Here, a 4th laser pulse can be used for time resolved optical pump-X-ray probe measurements. The forward scattering is recorded for crystallographic analysis (bottom left) while the X-ray emission signal (top left) is measured utilizing an energy dispersive spectrometer mounted above and a detector located sideways of the interaction point.

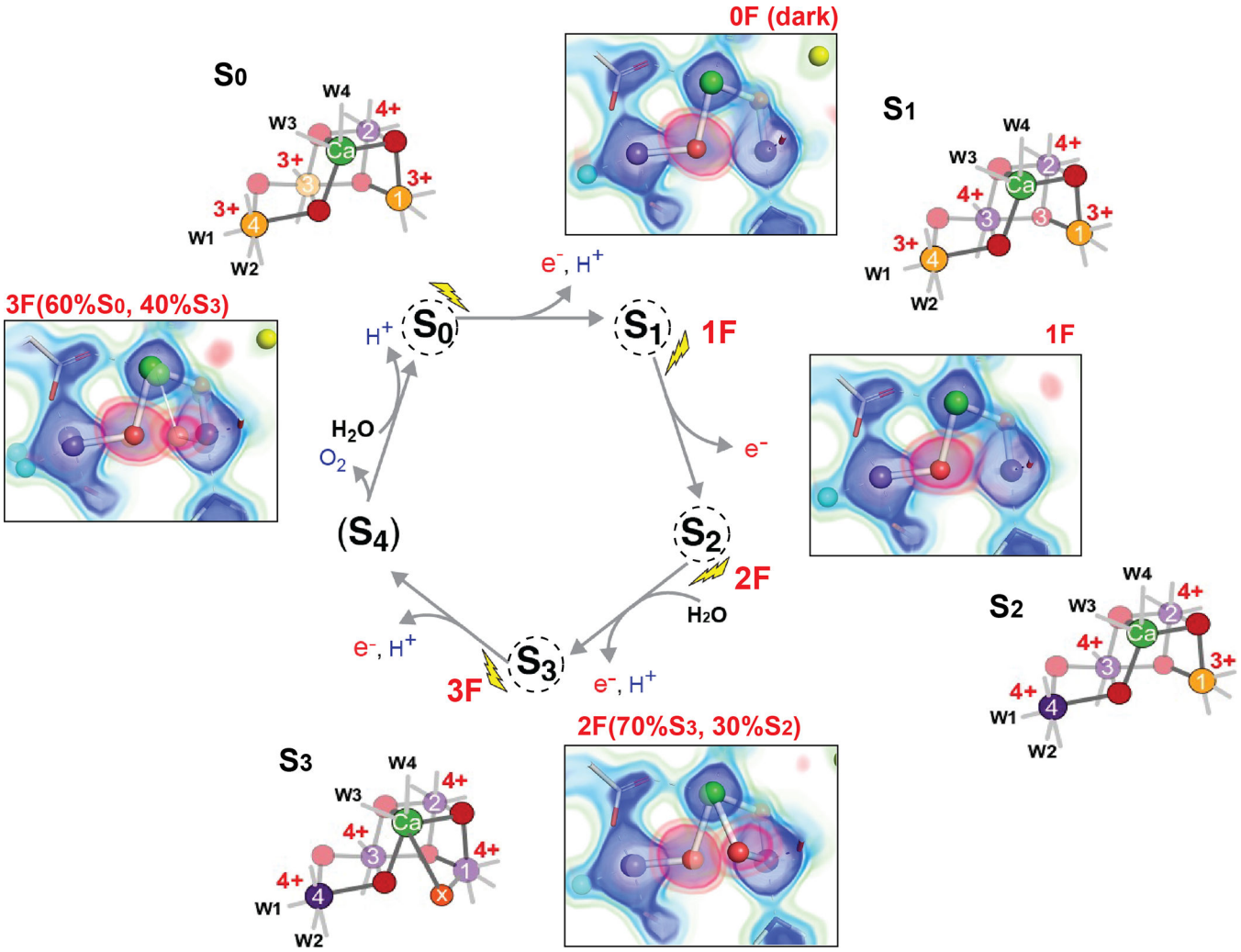

Figure 2. Kok cycle of the water oxidation reaction.

The reaction cycle of light-driven water oxidation in PS II is shown in the center. Starting in the dark stable S_1 state each light flash given to the system advances the Mn_4CaO_n cluster by one oxidation state with S_3 being the highest oxidized stable intermediate state. The next photon triggers the formation and release of O_2 via the transient S_4 state and relaxation of the cluster to the most reduced S_0 state which returns to the S_1 state by another light flash. Electron density ($2mF_{obs} - DF_{calc}$) at different contour levels (1.5, 3 and 4 σ, green to blue) and omit electron density ($mF_{obs} - DF_{calc}$, contoured at 3 (orange) and 4.5 σ (red)) for the O_5 and O_X oxygen atoms are shown together with structural models of the OEC in each of the S-states. Ca ligands are omitted for clarity. Adapted from [9].

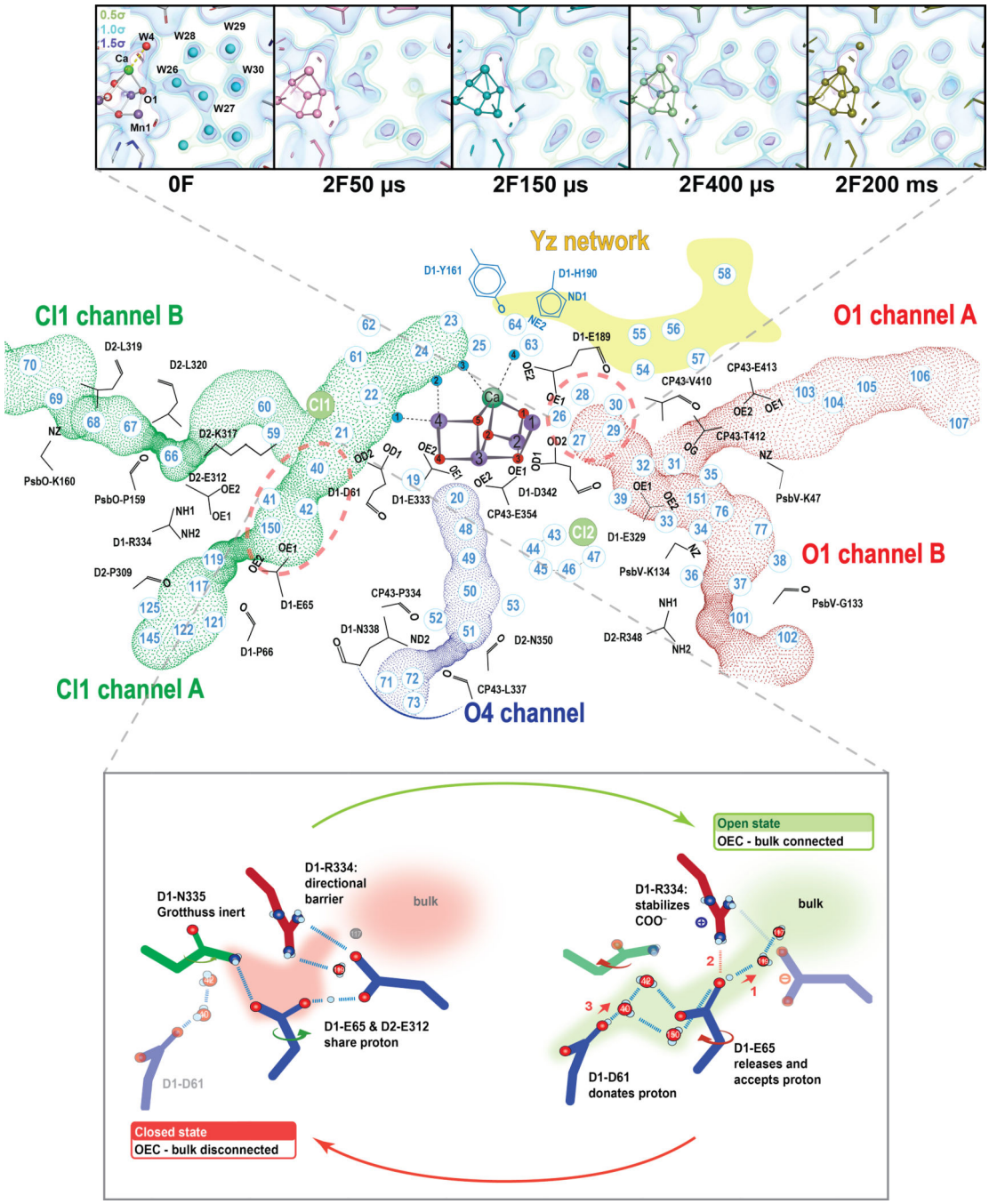

Figure 3. The environment of the Mn cluster in PSII.

The Mn_4CaO_n cluster (Mn shown as blue, Ca as green, oxygen as red spheres) is embedded in a network of water channels (**center**, adapted from [9]) connecting it to the bulk. The main channels are labelled ('O1 channel', 'O4 channel' and 'Cl1 channel'). Waters located in the room temperature X-ray structures are indicated by numbered circles and selected residues lining the channels are labeled. A pentamer of waters (W26-W30) located next to the O1 atom of the Mn cluster is indicated by a dashed circle. Changes in the electron density of this "water wheel" region at different time points in the S_2 to S_3 transition are

clearly visible (**top**, adapted from [8]). These indicate high water mobility and a possible role of the water wheel and the O1 channel in water transport to the Mn cluster related to the water insertion event that takes place upon formation of the S_3 state. A bottleneck in the Cl1 channel (highlighted by a dashed oval) changes configuration at around 150 μs into the S_2 to S_3 transition (**bottom**, adapted from [39]). This opening and closing of a potential "proton gate" could facilitate proton transfer from the cluster to the bulk during a specific time window in the S_2 to S_3 transition.